

Revealing the unseen: the organizer region of the nucleolus

Marco Biggiogera^{1,2,*}, Manuela Malatesta^{1,3,*}, Sousan Abolhassani-Dadras¹, François Amalric⁴, Lawrence I. Rothblum⁵ and Stanislav Fakan^{1,‡}

¹Centre of Electron Microscopy, University of Lausanne, 1005 Lausanne, Switzerland

²Dipartimento di Biologia Animale, Laboratorio di Istologia, and Centro di Studio per l'Istochimica del CNR, University of Pavia, 27100 Pavia, Italy

³Istituto di Istologia ed Analisi di Laboratorio, University of Urbino, 61029 Urbino, Italy

⁴Institut de Pharmacologie et de Biologie Structurale, CNRS, 31077 Toulouse, France

⁵Weis Center for Research, Geisinger Clinic, Danville, PA 17822, USA

*These authors contributed equally to this work

‡Author for correspondence (e-mail: sfakan@cme.unil.ch)

Accepted 22 May 2001

Journal of Cell Science 114, 3199-3205 (2001) © The Company of Biologists Ltd

SUMMARY

We carried out a high-resolution ultrastructural analysis of the nucleolus in mouse P815 cells by combining specific DNA and RNA staining, anti-fibrillar immunolabeling, contrast enhancement by energy filtering TEM and phosphorus mapping by ESI to visualize nucleic acids. We demonstrated that specifically contrasted DNA, fibrillar and phosphorus overlap within the nucleolar dense fibrillar component. Moreover, we describe a 'DNA cloud' consisting of an inner core of DNA fibers (fibrillar center) and a periphery made of extremely thin fibrils overlapping

the anti-fibrillar immunolabeling (dense fibrillar component). This highly sensitive approach has allowed us to demonstrate, for the first time, the exact distribution of DNA within the decondensed interphase counterpart of the NOR, which includes both the fibrillar center and the dense fibrillar component.

Key words: Nucleolus Organizer Region, Ultrastructure, Electron Spectroscopic Imaging, Immunocytochemistry

INTRODUCTION

Nucleolar organizer regions (NORs) are the metaphase chromosome regions in which rDNA is located. Although the number and the relative positions of NORs are known in metaphase chromosomes from different species, the exact location and arrangement of NORs in the nucleolus still remains to be elucidated. Silver staining techniques applied to interphase nucleoli result in the staining of two distinct nucleolar components (Moreno et al., 1985; Biggiogera et al., 1989): the fibrillar centre (FC) and the dense fibrillar component (DFC), whereas the granular component (GC) (see Jordan, 1984 for nucleolar component nomenclature) remains unstained. Because the GC does not contain DNA but only RNA and proteins within the preribosomal particles (Thiry and Goessens, 1996), the DNA-containing ribosomal genes must localize to the FC and/or the DFC. Various technical approaches at the electron microscopic level, such as autoradiography, in situ hybridization and immunocytochemistry, have been applied to solve the problem of the subcellular localization of the active rDNA genes but the question is still open after years of extensive investigation.

It seems to be clear that the unresolved problem consists of localizing, inside a complex and electron-dense structure such as the nucleolus, a small amount of DNA that, when transcribed, could be represented by very thin decondensed filaments. The real difficulty lies in the fact that the most dispersed portion of DNA (i.e. active genes) cannot be seen by conventional electron microscopy techniques in the

nucleolus in situ. In order to overcome these problems, we have developed a new approach by combining high-resolution immunocytochemistry and specific DNA and RNA staining with energy filtering transmission electron microscopy (EFTEM). This method, applied to mouse P815 cells, provides an extremely fine spatial resolution of single DNA molecules. The samples were observed after filtering inelastically scattered electrons, which, in a conventional transmission electron microscope (TEM), contribute to the formation of the background noise and thus could hide the thinner structures. Moreover, we have carried out phosphorus mapping in order to further confirm the exact location of the thin DNA fibrils found within the nucleolar components.

MATERIALS AND METHODS

Cell growth and fixation

Murine P815 cells were grown in Eagle's medium supplemented with 5% fetal calf serum and with penicillin and streptomycin. Before fixation, the cells were rinsed in Sørensen phosphate buffer (pH 7.3).

For the immunocytochemical procedures, the cells were fixed in 4% buffered paraformaldehyde for 2 hours at 4°C. After centrifugation (2000 rpm for 10 minutes at 4°C) and 2 hours of rinsing in buffer, they were incubated in aqueous 0.5 M NH₄Cl for 30 minutes at room temperature to block free aldehyde groups, rinsed again for 10-15 minutes in several changes of buffer and encapsulated in 2% low viscosity agarose. Dehydration in ethanol was carried out at

progressively lower temperatures and the cells were embedded in Lowicryl K4M at -35°C (Carlemalm et al., 1982).

For conventional morphology studies, the cells were fixed with 1.6% glutaraldehyde for 1 hour at 4°C followed by a post-fixation with 1% osmium tetroxide for 1 hour at room temperature. The samples were dehydrated in acetone and embedded in Epon.

Immunocytochemistry

An affinity-purified rabbit polyclonal antibody against *Xenopus* fibrillarin (Lapeyere et al., 1990) was diluted 1:100 and then reacted with goat anti-rabbit IgG coupled to 6 nm colloidal gold (Aurion, Wageningen, The Netherlands). A rabbit affinity purified antibody raised against RNA polymerase I (Hannan et al., 1998) was diluted 1:50 and then reacted with goat anti-rabbit IgG coupled with 15 nm colloidal gold (Jackson Laboratories, West Grove, PA).

Grids with thin sections were pre-incubated on droplets of normal goat serum diluted 1:100 in PBS for 3 minutes at room temperature. They were then floated for 17 hours at 4°C on the incubation mixture, consisting of the primary antibody and 0.1% bovine serum albumin (BSA, Sigma fraction V) in PBS containing 0.05% Tween 20 (Sigma). After rinsing with PBS-Tween and then PBS alone, the grids were placed onto droplets of the secondary antibody coupled to colloidal gold particles diluted in PBS for 30 minutes at room temperature. The grids were rinsed with PBS and water and finally air dried.

As a control for labeling specificity, some grids were treated with the incubation mixture from which the primary antibody was omitted. Some grids were then stained with uranyl acetate and lead citrate, and others were submitted to a cytochemical reaction (see below). The grids were observed with a Philips CM12 electron microscope, operated at 80 kV, using a 30-40 μm objective aperture.

DNA cytochemistry

For DNA specific staining, sections on gold grids were first floated on 5 N HCl for 20 minutes at room temperature, rinsed with water and then reacted with 0.1% osmium ammine solution (treated with SO_2) for 60 minutes at room temperature (Cogliati and Gautier, 1973; Olins et al., 1989). The sections were then rinsed with distilled water and dried.

In some cases, the grids were first labeled with the anti-fibrillarin antibody, revealed by 6 nm gold particles, and then stained with osmium ammine. As a control to check whether there was loss or displacement of the gold grains during the osmium ammine reaction, some grids were immunolabeled, hydrolyzed as above and then stained with uranyl acetate. Other grids were immunolabeled and stained with osmium ammine as above and subsequently post-stained with uranyl acetate and lead citrate.

RNA staining

In order to check whether RNA is removed by acid hydrolysis, sections (~ 70 nm thick) on gold grids were first floated on 5 N HCl for 3, 10 or 20 minutes at room temperature, rinsed with water and then stained with 0.2 M terbium citrate for 1 hour at room temperature, as described previously (Biggiogera and Fakan, 1998).

Energy dispersive analysis

We investigated whether terbium was present in the nucleoli specifically stained for RNA as above by means of energy dispersive analysis. Spectra were obtained using an EDAX system, which was installed on a Philips CM12 electron microscope operating at 80 kV. A probe size of ~ 500 nm was used and the analysis was performed at least on three different cells per sample, both on nucleoli and on the resin of the section (background).

Electron spectroscopic imaging

Ultrathin sections (~ 25 nm thick) were cut and collected onto 700-mesh hexagonal gold grids. After immunolabeling and osmium

amine staining, the grids were observed with a Zeiss CEM 902 transmission electron microscope equipped with a prism-mirror-prism electron spectrometer. The acceleration voltage of the microscope was 80 kV, the condenser aperture 600 μm , objective aperture 90 μm , spectrometer entrance aperture 100 μm and the slit size (energy selecting aperture) between 10 eV and 17 eV according to whether a contrast enhanced image or elemental mapping had to be performed. Image acquisition was accomplished with a Gatan 679 (Gatan Inc., Warrendale, PA) slow scan CCD camera (Krivanek and Mooney, 1993). Data collection and image treatment were carried out on a Power Macintosh computer using Gatan Digital Micrograph 2.5 software. Zero-loss filtered and 250 eV contrast enhanced images were used to reveal the fine structure of the nucleolar components. The net phosphorus distribution was calculated using a three-window method (Egerton 1986; Reimer et al., 1992; Bazett-Jones 1993) with the following windows: 102 eV and 122 eV for the two background readings, and 152 eV for the phosphorus $\text{L}_{2,3}$ edge. In this case the slit size was ~ 10 -12 eV. Once the map had been obtained, the images were normalized in order to enhance their contrast. In the phosphorus maps, the brighter regions of the image correspond to the structures with a higher concentration of this element. The pixel size in these images is 7.52 nm for the 12,000 \times images, 4.4 nm for the 20,000 \times images and 3.12 nm for the 30,000 \times images. The thickness of the specimen was controlled with a series acquired between 0 eV and 100 eV energy losses.

DFC and FC measurements

All measurements were carried out on paraformaldehyde-fixed Lowicryl-embedded samples. Twenty-five micrographs of both FC and DFC complexes from uranyl-lead stained samples and DNA clouds from osmium-amine-stained specimens were taken and printed at the same magnification (120,000 \times). FC and DNA cloud diameters and DFC thickness were measured and minimum and maximum values were considered.

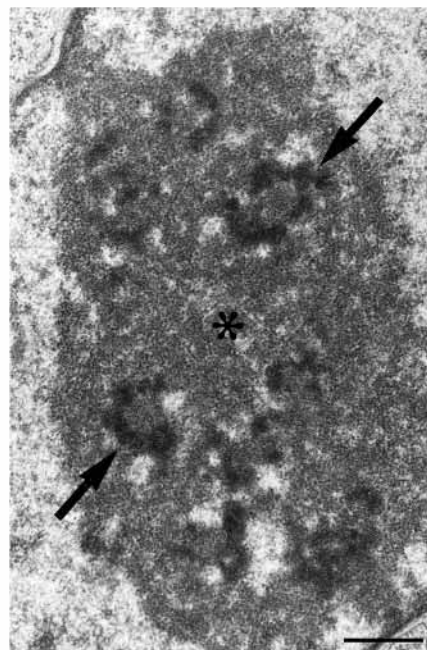


Fig. 1. Nucleolus of a mouse P815 cell. Glutaraldehyde-osmium fixation, Epon embedding, uranyl-lead staining. The DFC (arrows) appears as a strongly electron-dense structure surrounding the FCs. Most of the nucleolus is formed by the GC (asterisk). Bar, 0.5 μm .

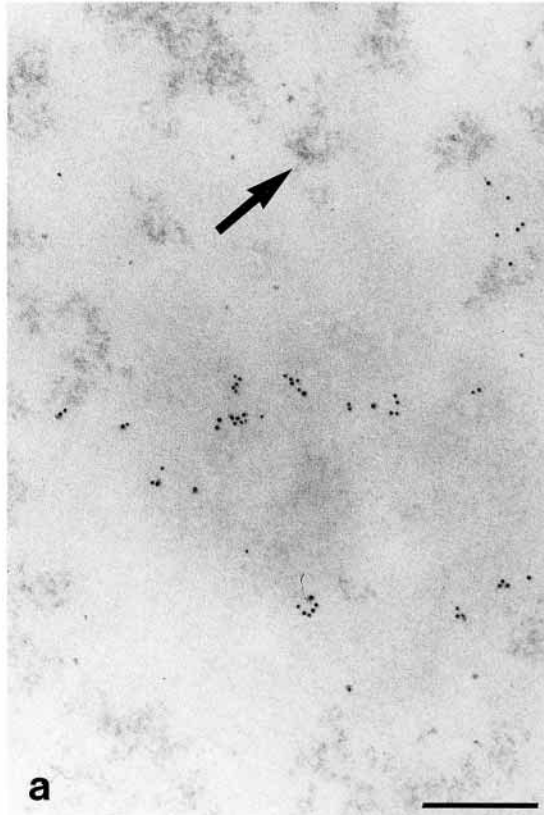
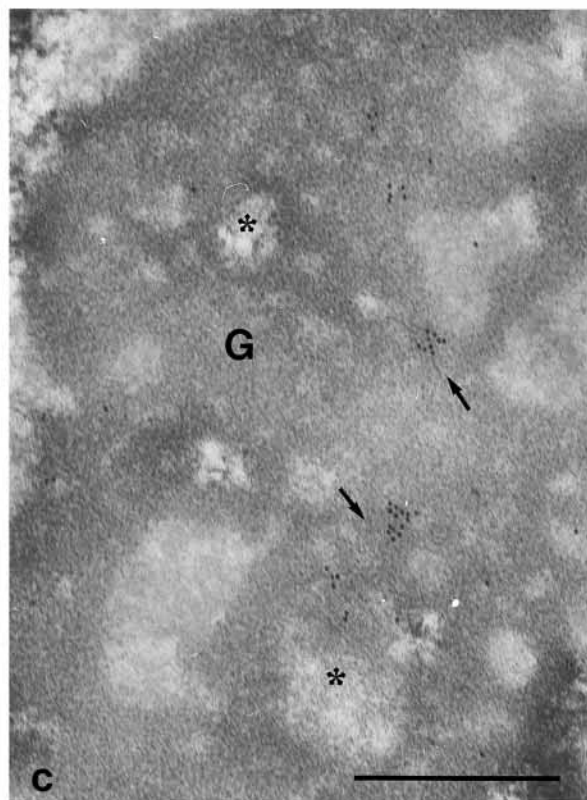
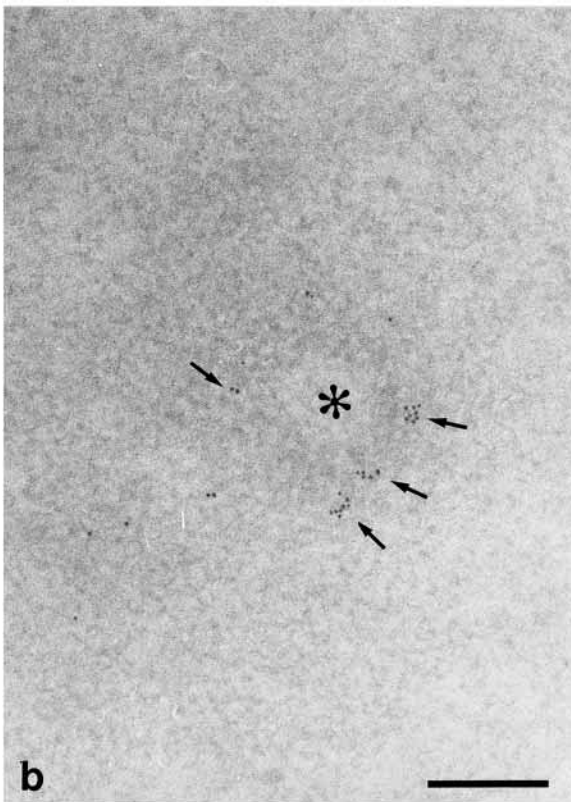


Fig. 2. (a) Immunolabeling for fibrillar and specific DNA staining with osmium ammine. The labeling for fibrillar, a marker of the DFC, is present at the periphery of a stained area formed by thin fibers of DNA. Clumps of intranucleolar chromatin are also stained (arrow). Notice that the different nucleolar components shown in Fig. 1 are no more recognizable. Bar, 0.2 μm . (b) Control sample submitted to anti-fibrillar labeling, hydrolysis with 5 N HCl for 20 minutes and staining with uranyl acetate. The DFC surrounding the FC (asterisk) is specifically labeled (arrows). Bar, 0.2 μm . (c) After immunolabeling with an anti-RNA-polymerase-I antibody, the gold particles are located over the DFC (arrows). The FCs (asterisks) and the GC (G) are devoid of labeling. Bar, 0.5 μm .



RESULTS

In interphase nucleoli, the DFC appears as a strongly electron-dense rim surrounding a rounded finely fibrillar area

corresponding to the FC, as seen on conventionally contrasted electron microscopic specimens (Fig. 1). However, when the Feulgen-type osmium ammine reaction, specific for DNA, is carried out, nucleoli appear as electron-lucent areas in which

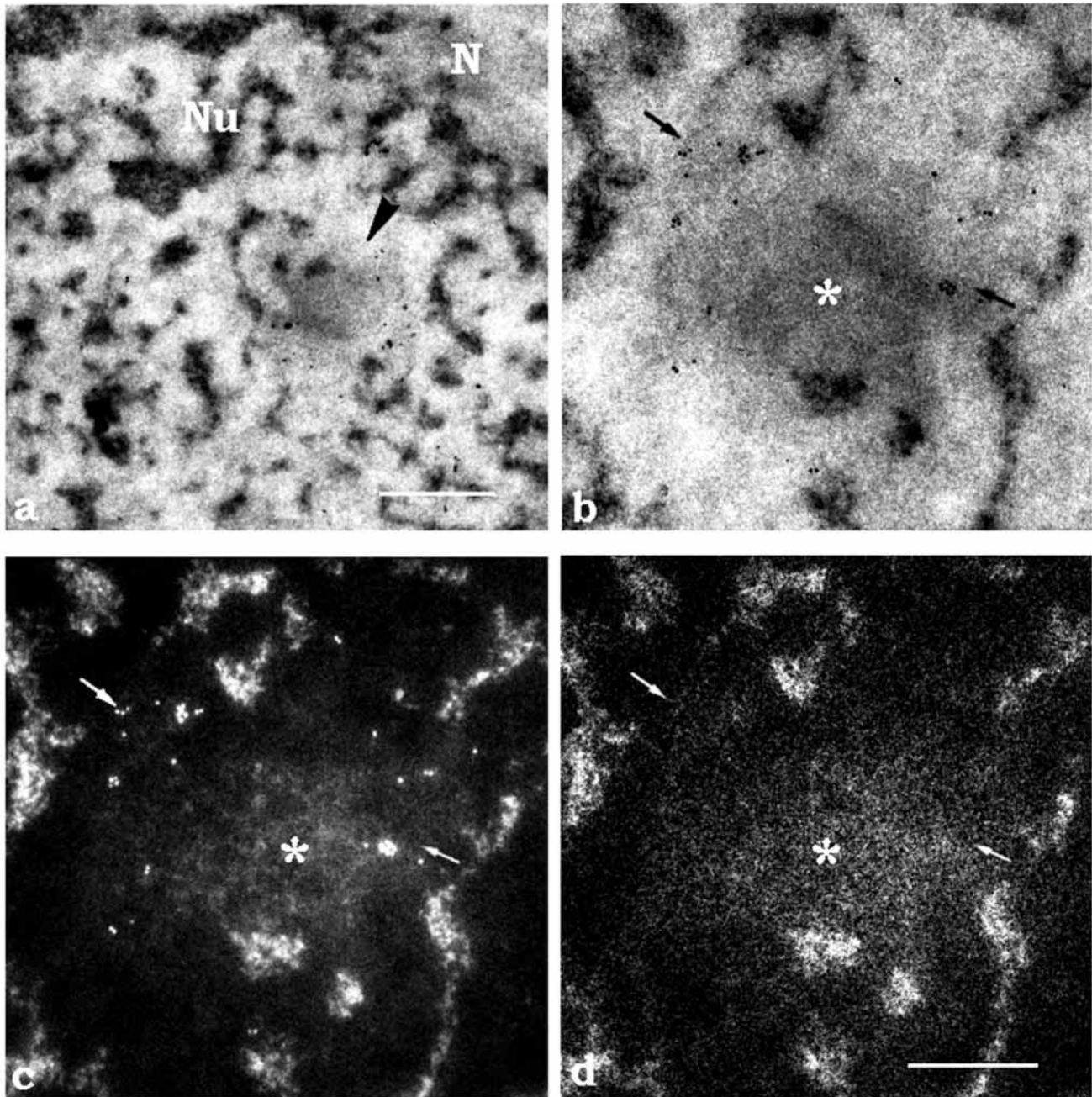


Fig. 3. (a) Ultrathin (25 nm) section through a nucleolus immunolabeled as in Fig. 2 and stained for DNA. Observation at 0 eV loss. Under these conditions, the nucleolus (Nu) appears as an 'empty' area in which DNA fibers are present as clumps scattered in the nucleolar body. A cloud of thin DNA fibers, the periphery of which overlaps the anti-fibrillarin labeling, can be seen in the center (arrowhead). Abbreviation: N, nucleoplasm. Bar, 0.5 μ m. (b) At a higher magnification, it is clearly evident that the gold grains localizing fibrillarin are present at the periphery of the cloud (asterisk) and superimposed on the thinner fibers within the external part of the DNA cloud (arrows). (c) The same area as in b, observation at 250 eV energy loss. At this energy loss, it is clear that the inner core of the DNA cloud (asterisk) is formed by fibers thinner than chromatin clumps but thicker than those overlapping the anti-fibrillarin labeling (arrows). (d) The same area as in b and c, after phosphorus mapping. Phosphorus is present in all the locations that were positive in the DNA staining. Even the thin filaments at the periphery of the cloud are visible (arrows). Bar, 0.2 μ m.

the differences between the DFC, GC and FC are lost (Fig. 2). For this reason, a simultaneous visualization of fibrillarin, a marker protein present only in the DFC, is mandatory in order to determine the relative position between the osmium-amine-stained DNA and this nucleolar component. After labeling with anti-fibrillarin antibody followed by osmium

amine contrasting, some fibers of stained DNA are observed in the areas where the gold grains also occur (Fig. 2a). Control specimens show that the gold grains were neither displaced nor removed during the Feulgen reaction, thus confirming the reliability of the technique (Fig. 2b). Furthermore, after immunolabeling with anti-RNA polymerase I antibodies, most

signal occurs in the DFC (Fig. 2c), thus confirming some (Raska et al., 1995; Cmarko et al., 2000) but not all (Scheer and Rose, 1984) previous results.

The contrast obtained when observing osmium ammine-stained specimens by conventional electron microscopy is weak and can be increased by the contrast enhancement obtained by energy filtration TEM (EFTEM) at 0 eV loss. In this way, when filtering the inelastically scattered electrons, even the thinner DNA fibers become visible both within and in the vicinity of fibrillar-containing DFC (Fig. 3a,b). Anti-fibrillar immunolabeling is frequently present at the periphery of rounded areas consisting of a 'cloud' of stained DNA. This weakly electron-dense peripheral region is made up of thin DNA fibers, whereas the central part shows a stronger electron density. In addition, the DNA clouds are always in continuity with two or more intranucleolar chromatin clumps (Fig. 3b). Measurements made on micrographs of conventionally stained nucleoli demonstrate that the diameter of the FC ranges from 0.24 μm to 0.32 μm , whereas that of the complex of FC and DFC range from 0.41 μm to 0.51 μm . When the samples are specifically stained for DNA, the diameter of the DNA cloud as seen at 0 eV loss ranges between 0.39 μm and 0.46 μm . The morphometrical data therefore confirm that the DNA cloud is always larger than the FC alone, overlapping the DFC domain, and that the DNA within the DFC is formed by the most dispersed part of the cloud.

Observation of sections at an electron energy loss of 250 eV, situated just before the carbon k-edge, reveals the finest details of general structure of the specimen (Reimer et al., 1992). Although we do not obtain any analytical indication at this energy loss, such images provide information that could otherwise be masked by the presence of heavy metals on conventionally stained specimens (Abolhassani-Dadras et al., 1994). Thus, in Fig. 3c, the DNA thin fibrils appear clearly inside the DFC whereas the thickest DNA bundles occur within the cloud core, which corresponds to the FC.

Phosphorus mapping (Fig. 3d) on the same nucleolar area indicates that P exactly matches the osmium-ammine-stained DNA within the cloud as well as in the clumps of condensed chromatin; under these conditions, the signal owing to phosphorus comes from DNA because RNA, as other major source of phosphorus signal, has been degraded and removed by the acid hydrolysis step preceding the osmium ammine reaction. In order to ascertain that RNA is actually lost during the hydrolysis, we used the terbium citrate technique (Biggiogera and Fakan, 1998) as a specific high-resolution stain for RNA after different periods of HCl treatment. This demonstrated that some terbium-contrasted RNA is still present after 10 minutes HCl treatment but that, after 20 minutes, no detectable RNA was observed within the nucleolus. These results were confirmed by energy dispersive analysis of the samples: terbium could not be identified after 20 minutes of hydrolysis (not shown). In control sections (submitted first to hydrolysis and osmium ammine staining, and then post-stained with uranyl acetate and lead citrate), the final contrast of the nucleolar components was strongly decreased when compared with that of non-hydrolyzed sections. This means that most proteins, another possible source of phosphorus signal, have been lost during the HCl treatment. Importantly, we have been able to remove RNA and

proteins from a 70 nm section, which is at least three times thicker than those used for phosphorus mapping.

DISCUSSION

The question of the precise location of interphase NOR and, in particular, of rDNA expression inside the nucleolar components has long been a matter of debate. Of the four components of the nucleolus (DFC, FC, GC and chromatin), the GC (which contains the pre-ribosomal particles and no DNA) is the last to form in a newly formed nucleolus, whereas the NOR chromatin (which contains the ribosomal genes) is the first as well as the basis of the nucleolus. Therefore, transcription takes place within one of the two remaining nucleolar components, DFC and FC, where the rDNA occurs. Moreover, the DFC and FC are the nucleolar components stained with silver similarly to NORs in the metaphase chromosomes. However, efforts to localize the ribosomal transcribing genes within these two nucleolar components gave rise to contradictory results, some data suggesting the presence of ribosomal genes in the DFC (Wachtler et al., 1989; Stahl et al., 1991; Jimenez-Garcia et al., 1993; Hozak, 1995), others in the FC (Derenzini et al., 1982, 1985; Thiry and Thiry-Blaise, 1991) and some in both compartments (Puvion-Dutilleul et al., 1991; Thiry and Goessens, 1996).

Our novel approach making use of a combination of several complementary high resolution ultrastructural techniques (cytochemistry, immunocytochemistry, EFTEM and ESI) has allowed for the first time both the visualisation and the localisation of DNA containing ribosomal genes in its most finely dispersed form within a precise nucleolar components. We have thus demonstrated, first, that the specifically stained DNA, the immunolabeling for the DFC marker protein fibrillar and for RNA polymerase I, and the phosphorous signal obtained by ESI overlap within the same nucleolar area. This demonstrates the presence of DNA inside the DFC of mouse P815 cell nucleoli. Second, stained DNA often occurs as clouds, with an inner core of DNA fibers obviously corresponding to the FC. This disentangles at its periphery into extremely thin fibrils overlapping the immunolabeling for fibrillar (DFC). The FC+DFC complex therefore represents the decondensed interphase counterpart of the NOR.

The DFC contains finely dispersed DNA

Our combined approach, based on the possibility of obtaining different kinds of information on exactly the same nucleolar area, allowed us unambiguously to demonstrate the presence of finely dispersed DNA fibrils within the DFC. The anti-fibrillar immunolabeling permits a precise localization of the DFC, overcoming the technical problems linked to the hydrolysis step of the Feulgen-type reaction, which, by removing RNA and proteins, makes it difficult to recognize the different nucleolar components. In addition, the observation at 0 eV enhances the contrast of osmium-ammine-stained DNA, the observation at 250 eV helps to visualize the DNA fibrillar structure and the phosphorus map, overlapping with the data obtained at 0 eV energy loss, confirms the presence of finely dispersed DNA fibrils in the DFC. The phosphorus signal comes from DNA because we have demonstrated that RNA, the other major source of phosphorus signal, is degraded by

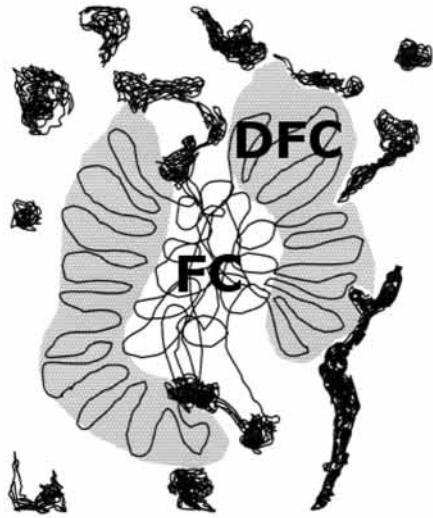


Fig. 4. Schematic interpretation of Fig. 3b-d. The DNA cloud originates in the peripheral clumps of condensed chromatin, forms the FC (intermediate step of uncoiling) and expands to form the DFC (thinnest DNA fibers, active genes). The gray areas represent the zone labeled by the anti-fibrillarin antibody. The DNA cloud and the condensed chromatin from which it originates correspond to the interphase NOR.

acid hydrolysis and lost. Proteins, another possible source of phosphorus signal, are mostly removed during the HCl treatment, as testified by the evident loss of electron density of the nucleolar components. Furthermore, we have direct evidence that, when hydrolysis is carried out in vapor phase (i.e. grids are not in contact with HCl aqueous solution), proteins are retained within the nucleolus and the different nucleolar components keep their inherent contrast (Biggiogera and Fakan, unpublished).

DNA clouds correspond to the FC+DFC complex

We have found that osmium-amine-stained DNA inside the nucleolus occurs as rounded clouds made of fibrils thinner than those present in the clumps of condensed chromatin. Similar areas of decondensed DNA have been reported previously (Derenzini et al., 1982; Derenzini et al., 1987; Derenzini et al., 1993) and interpreted as highly dispersed DNA within the FC, whereas the DFC was considered to be devoid of DNA. However, our combined, highly sensitive approach shows that the osmium-amine-stained DNA described by these authors represented only the most contrasted inner part of the DNA cloud revealed in the present work; the peripheral part, located in the DFC, was not visible or only barely detectable by means of conventional electron microscopy. Therefore, the DNA cloud is formed by the FC+DFC complex, which represents the decondensed interphase counterpart of the NOR.

NOR and transcription sites

The pathway of NOR DNA decondensation leading towards transcribing genes proceeds through three steps of uncoiling, represented by intranucleolar chromatin, FC and DFC, respectively (Fig. 4). In fact, our results demonstrate that DNA distribution within the clouds is not homogeneous, the DNA present in the DFC being in filaments thinner than those

present in the FC. This suggests a degree of uncoiling, corresponding to active genes. This idea is supported by the following data. Fibrillarin, a component of the nucleolar U3 snRNP complex, involved in several steps of pre-rRNA-processing pathway and, in particular, in its early events (Kass et al., 1990) occurs in the DFC similarly to nucleolin and B23 protein (Biggiogera et al., 1989), UBF (Cmarko et al., 2000), and the ribosomal proteins P1P2 and L7 (Biggiogera et al., 1990), which become associated rather early with the nascent transcript (Chooi and Leiby, 1981; Ginisty et al., 1998). The presence of RNA polymerase I has also been reported in the DFC (Raska et al., 1995; Cmarko et al., 2000; this study). The DFC is also the site of occurrence of rapidly labeled RNA after ^3H -uridine incorporation (Granboulan and Granboulan, 1965; Fakan and Puvion, 1980; Fakan, 1986; Hozak, 1995) as well as after BrUTP incorporation (Cmarko et al., 1999; Cmarko et al., 2000), and transcribing genes have been detected in this nucleolar component by in situ hybridization (Wachtler et al., 1989; Stahl et al., 1991). In addition, if we consider that the transcripts and the transcription machinery constitute a relatively high density assembly and that the DFC is the most electron-dense nucleolar component, the DFC obviously corresponds to the actual site of transcription of ribosomal genes. By contrast, the FC is formed by DNA that is more condensed than that of DFC but less condensed than that of perinucleolar or intranucleolar chromatin masses. Our interpretation is supported by the analysis of neuron nucleoli during the circadian cycle (Pébusque and Seite, 1981), demonstrating variations in size of the FC. The enlargement of this compartment during the active period suggests that the DFC is proportionally much larger and that the DNA cloud is more dispersed. This leads to the conclusion that the genes are in a much more favorable arrangement for their expression.

Although the DFC is always present in all cells, FCs are hardly or not identifiable in rare cell types. Consequently, the FCs are either very small or the DNA containing ribosomal genes to be transcribed is directly released from intranucleolar condensed chromatin areas (always associated with the DFC) without uncoiling through an intermediary form of DNA condensation corresponding to FCs.

In conclusion, the DNA cloud corresponds to the decondensed interphase NOR and contains the FC+DFC complex. We hence define the FC and DFC as being the morphological expression of inactive and active rDNA genes, respectively.

We wish to thank J. Fakan for excellent technical assistance and L. Sagalowicz and F. Ardizzoni for the energy dispersive analysis. This work was supported by the Swiss National Science Foundation (grants 31.43333.95 and 31.53944.98 to S.F.), and grants from NIH (GM 46991) and Geisinger Foundation to L.I.R. M.B. and M.M. were recipients of a fellowship from CNR-FNRS (Accordo di cooperazione scientifica, 132.19.2-040651 and 132.19.2-040648).

REFERENCES

- Abolhassani-Dadras, S., Vázquez-Nin, G. H., Echeverría, O. M., Boutinard Rouelle-Rossier, V. and Fakan, S. (1994). ESI in situ analyses of extrachromosomal RNP granules. *J. Microsc.* **174**, 233-238.
- Bazett-Jones, D. P. (1993). Empirical basis for phosphorus mapping and structure determination of DNA:protein complexes by electron spectroscopic imaging. *Microbeam Anal.* **2**, 69-79.

- Biggiogera, M. and Fakan, S.** (1998). Fine structural specific visualization of RNA on ultrathin sections. *J. Histochem. Cytochem.* **46**, 389-395.
- Biggiogera, M., Fakan, S., Kaufmann, S. H., Black, A., Shaper, J. H. and Busch, H.** (1989). Simultaneous immunoelectron microscopic visualization of protein B23 and C23 distribution in the HeLa cell nucleolus. *J. Histochem. Cytochem.* **37**, 1371-1374.
- Biggiogera, M., Fakan, S., Leser, G., Martin, T. E. and Gordon, J. E.** (1990). Immunoelectron microscopic visualization of ribonucleoproteins in the chromatoid body of mouse spermatids. *Mol. Reprod. Dev.* **26**, 150-158.
- Carlemalm, E., Garavito, R. M. and Villiger, W.** (1982). Resin development for electron microscopy and an analysis of embedding at low temperature. *J. Microsc.* **126**, 123-143.
- Chooi, W. Y. and Leiby, K. R.** (1981). An electron microscopic method for localization of ribosomal proteins during transcription of ribosomal DNA: a method for studying protein assembly. *Proc. Natl. Acad. Sci. USA* **78**, 4823-4827.
- Cogliati, R. and Gautier, A.** (1973). Mise en évidence de l'ADN et des polysaccharides à l'aide d'un nouveau réactif 'de type Schiff'. *C. R. Acad. Sci.* **276**, 3041-3044.
- Cmarko, D., Verschure, P. J., Martin, T. E., Dahmus, M. E., Krause, S., Fu, X. D., van Driel, R. and Fakan, S.** (1999). Ultrastructural analysis of transcription and splicing in the cell nucleus after BrUTP-microinjection. *Mol. Biol. Cell* **10**, 211-223.
- Cmarko, D., Verschure, P. J., Rothblum, L. I., Hernandez-Verdun, D., Amalric, F., van Driel, R. and Fakan, S.** (2000). Ultrastructural analysis of nucleolar transcription in cells microinjected with 5-bromo-UTP. *Histochem. Cell Biol.* **113**, 181-187.
- Derenzini, M., Hernandez-Verdun, D. and Bouteille, M.** (1982). Visualization in situ of extended DNA filaments in nucleolar chromatin of rat hepatocytes. *Exp. Cell Res.* **141**, 463-469.
- Derenzini, M., Pession, A. and Licastro, F. E. A.** (1985). Electron-microscopical evidence that ribosomal chromatin of human circulating lymphocytes is devoid of histones. *Exp. Cell Res.* **157**, 50-62.
- Derenzini, M., Farabegoli, F., Pession, A. and Novello, F.** (1987). Spatial redistribution of ribosomal chromatin in the fibrillar centres of human circulating lymphocytes after stimulation of transcription. *Exp. Cell Res.* **170**, 31-41.
- Derenzini, M., Farabegoli, F. and Trerè, D.** (1993). Localization of DNA in the fibrillar components of the nucleolus - a cytochemical and morphometric study. *J. Histochem. Cytochem.* **41**, 829-836.
- Egerton, R. F.** (1986). In *Electron Energy-Loss Spectroscopy in the Electron Microscope*, pp. 255-262. New York: Plenum Press.
- Fakan, S.** (1986). Structural support for RNA synthesis in the cell nucleus. In *Nuclear Submicroscopy* (eds G. Jasmin and R. Simard), pp. 105-140. Basel: Karger.
- Fakan, S. and Puvion, E.** (1980). The ultrastructural visualization of nucleolar and extranucleolar RNA synthesis and distribution. *Int. Rev. Cytol.* **65**, 255-299.
- Ginisty, H., Amalric, F. and Bouvet, P.** (1998). Nucleolin functions in the first step of ribosomal RNA processing. *EMBO J.* **17**, 1476-1486.
- Granboulan, N. and Granboulan, P.** (1965). Cytochimie ultrastructurale du nucléole. II. Etude des sites de synthèse du RNA dans le nucléole et le noyau. *Exp. Cell Res.* **38**, 604-619.
- Hannan, R., Hempel, W. M., Cavanaugh, A., Arino, T., Dimitrov, S.I., Moss, T. and Rothblum, L.** (1998). Affinity purification of mammalian RNA polymerase I. *J. Biol. Chem.* **273**, 1257-1267.
- Hozak, P.** (1995). Catching RNA polymerase I in Flagranti: ribosomal genes are transcribed in the dense fibrillar component of the nucleolus. *Exp. Cell Res.* **216**, 285-289.
- Jimenez-Garcia, L. F., Segura-Valdez, M. D., Ochs, R. L., Echeverria, O. M., Vazquez-Nin, G. H. and Busch, H.** (1993). Electron microscopic localization of ribosomal DNA in rat liver nucleoli by nonisotopic in situ hybridization. *Exp. Cell Res.* **207**, 220-225.
- Jordan, E. G.** (1984). Nucleolar nomenclature. *J. Cell Sci.* **67**, 217-220.
- Kass, S., Tyc, K., Steitz, J. A. and Sollner-Webb, B.** (1990). The U3 small nucleolar ribonucleoprotein functions in the 1st step of preribosomal RNA processing. *Cell* **60**, 897-908.
- Krivanek, O. L. and Mooney, P. E.** (1993). Application of slow-scan CCD cameras in transmission electron microscopy. *Ultramicroscopy* **49**, 95-108.
- Lapeyere, B., Mariottini, P., Mathieu, C., Ferrer, B., Amaldi, F., Amalric, F. and Caizergues-Ferrer, M.** (1990). Molecular cloning of *Xenopus* fibrillarin, a conserved U3 small nuclear ribonucleoprotein recognized by antisera from humans with autoimmune disease. *Mol. Cell Biol.* **10**, 430-434.
- Moreno, F. J., Hernandez-Verdun, D., Masson, C. and Bouteille, M.** (1985). Silver staining of the nucleolar organizer regions (NORs) on Lowicryl and cryo-ultrathin sections. *J. Histochem. Cytochem.* **33**, 389-399.
- Olins, A. L., Moyer, B. A., Kim, S. H. and Allison, D. P.** (1989). Synthesis of a more stable osmium ammine electron dense stain. *J. Histochem. Cytochem.* **37**, 395-398.
- Pébusque, M.-J. and Seïte, R.** (1981). Electron microscopic studies of silver-stained proteins in nucleolar organizer regions: location in nucleoli of rat sympathetic neurons during light and dark periods. *J. Cell Sci.* **51**, 85-94.
- Puvion-Dutilleul, F., Bachelierie, J. P. and Puvion, E.** (1991). Nucleolar organization of HeLa cells as studied by in situ hybridization. *Chromosoma* **100**, 395-409.
- Raska, I., Dunder, M., Koberna, K., Melcak, I., Risueno, M. C. and Torok, I.** (1995). Does the synthesis of ribosomal RNA take place with nucleolar centers or dense fibrillar components? A critical appraisal. *J. Struct. Biol.* **114**, 1-22.
- Reimer, L., Fromm, I., Hirsch, P., Plate, U. and Rennekamp, R.** (1992). Combination of EELS modes and electron microscopic imaging and diffraction in an energy filtering electron microscope. *Ultramicroscopy* **46**, 335-347.
- Scheer, U. and Rose, K. M.** (1984). Localization of RNA polymerase I in interphase cells and mitotic chromosomes by light and electron microscopic immunocytochemistry. *Proc. Natl. Acad. Sci. USA* **81**, 1431-1435.
- Stahl, A., Wachtler, F., Hartung, M., Devictor, M., Schöfer, C., Mosgöller, W., de Lanversin, A., Fouet, C. and Schwarzacher, H. G.** (1991). Nucleoli, nucleolar chromosomes and ribosomal genes in the human spermatocyte. *Chromosoma* **101**, 231-244.
- Thiry, M. and Thiry-Blaise, L.** (1991). Locating transcribed and non-transcribed rDNA spacer sequences within the nucleolus by in situ hybridization and immunoelectron microscopy. *Nucleic Acids Res.* **19**, 11-15.
- Thiry, M. and Goessens, G.** (1996). *The Nucleolus During the Cell Cycle*. Berlin: Springer-Verlag
- Wachtler, F., Hartung, M., Devictor, M., Wiegant, J., Stahl, A. and Schwarzacher, H. G.** (1989). Ribosomal DNA is located and transcribed in the dense fibrillar component of human Sertoli cell nucleoli. *Exp. Cell Res.* **184**, 61-71.